FIBRE OPTIC SENSORS FOR IMPACT-INDUCED DAMAGE DETECTION AND ASSESSMENT IN COMPOSITE MATERIALS

Leonidas Dokos [1], *Matthew Mowlem* [1], *Dr Alan Chambers* [1] *and Gilberto Brambilla* [2]
[1] Department of Engineering Materials, University of Southampton,
[2] Optoelectronics Research Centre, University of Southampton,
Southampton, United Kingdom (SO17 1BJ)

ABSTRACT: Low velocity impact (LVI) is considered potentially dangerous for a composite structure mainly because the damage, in the form of delaminations and matrix cracking, is created within the laminate or near the back face and might be left undetected. Most of the conventional damage assessment techniques require the composite structure or component to be taken out of service. A novel in-situ damage monitoring system using embedded fibre optic sensors was employed to study LVI and to perform impact damage assessment together with an instrumented falling dart impact tester. In this study, the impact energy varied by adjusting the drop heights.

KEYWORDS: Composite Materials, Carbon/Epoxy Laminate, Low Velocity Impact, Impact Damage, Detection, Assessment, Fibre Optic Sensors, Residual Strains, Fibre Bragg Gratings

INTRODUCTION

Composite materials are widely used in aircraft, modern vehicles and lightweight structures. They have a high strength-to-weight and stiffness-to-weight ratio but the mismatch in engineering properties through the thickness of laminated composites makes them susceptible to impact damage. Low velocity impact is considered potentially dangerous for a composite structure mainly because the damage may not be visible on the laminate surface and therefore might be left undetected. In many situations, the level of impact at which visible damage is formed is much higher than the level at which substantial loss of residual properties occurs [1]. Low velocity impact may be caused during manufacture, by careless handling, or during service and maintenance perhaps by accidentally dropped tools on the structure.

In order to assess the damage, the 'conventional' techniques of non-destructive evaluation (NDE) are not well suited for real time monitoring. All these methods require the structure to be taken out of service and often disassembled. This approach is uneconomical and sometimes impossible to implement [2]. Therefore there is a lack of practical inspection methods for composite structures and this is currently a major restriction to the most efficient use of composites. An efficient method needs to be quick, reliable and low-cost. It would permit the early detection of internal damage, which is below or at the Barely Visible Impact Damage (BVID). The BVID condition is that at which damage is just detectable upon careful visual inspection [3]. Nevertheless it reduces severely the structural integrity of the composite structure [4].

Damage detection using fibre optic sensors (FOS) offers the possibility of changing, with moderate

effort in weight and cost, the inspection and maintenance philosophy of modern composite structures. Optical fibres have dimensional similarity with the reinforcing fibres of a composite, are small in size, corrosion free and immune to electro magnetic interference (EMI). They are also sensitive to several kinds of parameters, such as temperature, strain and pressure. In the recent years, several schemes of damage detection using optical fibre sensors have been investigated. However, few of the efforts to develop an optical fibre sensor system for impact applications can be considered fully successful [5] due to the significant technical challenges facing the use of fibre optic sensors.

This paper presents an experimental work accomplished by a newly developed interrogation system using fibre Bragg grating sensors (FBGS) together with an instrumented impact tester. The impact data from LVI tests on the carbon fibre reinforced panels (CFRP) are presented and discussed. The results from the fibre Bragg grating sensors were compared to those given by resistance strain gauges (RSG) and ultrasonic C-scanning. All the methods present great similarities in the detection of the impact event. The assessment of the impact-induced damage in the CFRP was impossible under the BVID condition using the strain gages or the C-scanning, while the FOS produced results underlining the existence of internal damage. A control group of composite panels without embedded optical fibre sensors is also tested under low velocity impacts to determine if an embedded optical fibre alters the structural integrity of composite plates during low velocity impacts.

THE FBGS TECHNOLOGY

A fibre optic Bragg grating is a periodic variation in the index of refraction along a certain length of the core of a single-mode optical fibre. This periodic structure makes the grating act as a wavelength-selective reflector. The centre wavelength of this reflection spike is determined by the Bragg relation $\lambda_0=2n_1\Lambda$, where Λ is the period of this index modulation and n_1 is the average refractive index of the fibre core. The strain response arises due to the physical elongation of the sensor (and corresponding fractional change in grating pitch) and the change in fibre index due to photo elastic effects [6]. Once the grating is subject to a strain, both the grating period length and the average refractive index will change and so accordingly will the reflective wavelength (Figure 1).

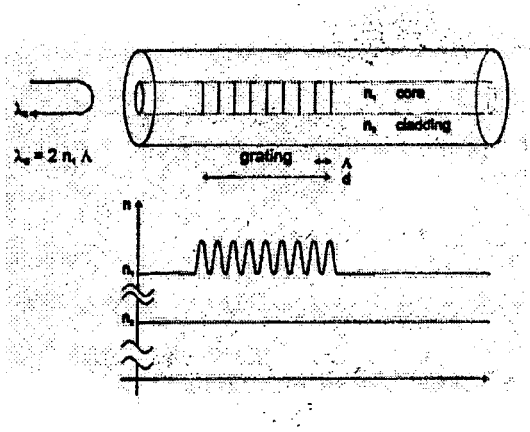

Fig. 1. Fibre Bragg grating sensor

The nature of Bragg gratings output provides these sensors with a built-in self-referencing capability. As the sensed information is encoded directly into wavelength, which is an absolute parameter, the output does not depend directly on the total light level, losses in the connecting fibres and couplers or source power. This is widely acknowledged as one of the most important advantages

of these sensors [7,8]. In addition, they are ideal for remote sensing and the wavelength-encoded nature of the output facilitates wavelength-division multiplexing (WDM) by allowing each sensor to be assigned to a different part of the available source spectrum and provide an array of sensors on a single fibre. Gratings at different wavelengths may be both situated along one fibre, or on different fibres.

The fibre Bragg grating sensors are ideally suited for deployment in advanced fibre-reinforced composite structures because of their small size and ease of integration into composite materials with minimal perturbation to the reinforcing fibres [9]. A masked UV beam is used to produce our fibre Bragg gratings. The advantages of the mask technique are its simplicity and that it does not require a narrowband laser source for high temporal coherence. This technique offers also the large potential for repeatable mass-produced gratings.

MANUFACTURE OF THE SAMPLES

For the manufacturing of the samples pre-impregnated high modulus carbon tape was used with an epoxy resin type 919HF-42%-M40B supplied by Cytec Fiberite Ltd. All specimens consisted of twenty layers and had dimensions 200 mm x 90 mm x 2mm. They were manufactured using identical resins and hand lay-up process. Eight of them incorporated the fibre optic sensors and had a lay-up of [0/90 $_2$/0/90/0{FOS}/0/90 $_2$/0 $_2$/90 $_2$/0 $_2$/90/0/90 $_2$/0], where {FOS} represents the plane of embedding for the FBGS. The composite panels without FOS had a lay-up of [{0/90 $_2$/0/90/0 $_2$/90 $_2$/0}$_2$].

During manufacturing of the samples, the FBGS have to be embedded in the composite panels without being damaged especially during the curing cycle, in which a temperature up to 125°C and pressure of several bars is reached. The integration plane is situated at a specific depth, which determines the sensor sensitivity to damage created by the impacts. The depth and the orientation of the FBGS was chosen according to the existing literature referring to the optimum position of embedded FBGS [10-12] in order to avoid the local perturbation in the geometry of the structural fibres, which results in local waviness. The FBGS were embedded at the upper face of the internal skin during plate manufacture, parallel with adjacent structural fibres and before the curing process. The two spectrally multiplexed FBGS are located on the same optical fibre and operate at two different wavelengths of 1530 and 1545 nm respectively. In addition, three resistance strain gauges by Kyowa are bonded on the backside of the plate and beneath the FBGS. Two are placed longitudinally and one is placed perpendicularly. The detailed position of the sensors is shown on Figure 2.

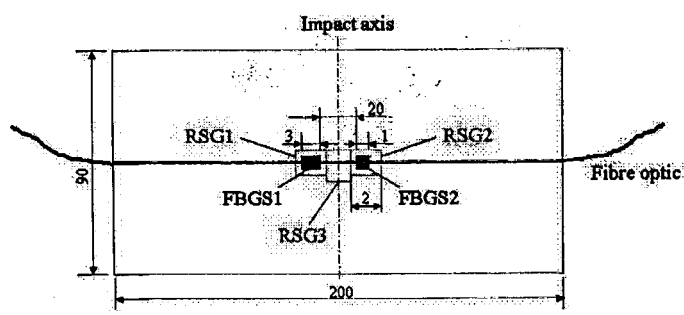

Fig. 2. Schematic diagram of the test coupon with the RSG and the embedded FBGS

EXPERIMENTAL SET-UP

An instrumented drop weight impact tower has been developed enabling low velocity impact tests to be conducted on clamped panels under similar test constraints shown in Figure 3. The drop-weight (0.359 kg) has an impactor with a hemi-spherical nose of 25 mm in diameter. The instrumented indentor is released from a predetermined height by a manual clutch. The specimens are clamped at all edges between two picture-frame plates with a circular opening of 60 mm in diameter. Re-strike of the drop weight is prevented by automatically covering the circular opening with a special designed mechanism exactly after the impact event.

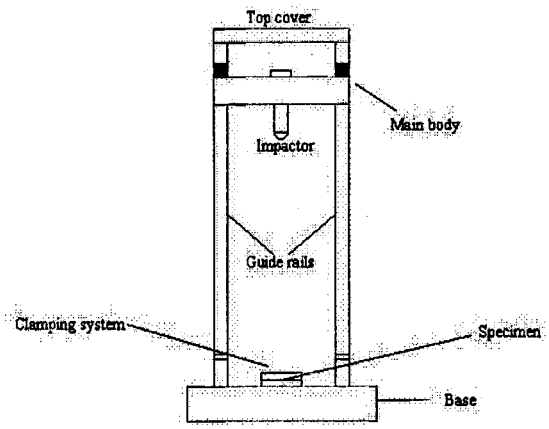

Fig 3. Schematic of the impact rig used for low velocity impact tests

The impactor is equipped with an accelerometer. It is a miniature piezoelectric transducer type 4369 by Brüel & Kjaer, which is connected via a Kistler Instruments charge amplifier type 5001 and a Bedo Elektronik signal conditioner to the data acquisition system. The accelerometer is attached inside the impactor nose for measuring the impact force imposed on the specimen. It has a charge sensitivity of 21.1 pC/g, a voltage sensitivity of 16.3 mV/g and a natural frequency of 36 kHz. In addition, a low-pass filter of 31 kHz is used to avoid high frequency alliasing of the accelerometer signal.

The resistance strain gauges by Kyowa are 2 mm long, and have a resistance of 350 Ω and a gage factor of 2. They are connected to an amplifier system model 2100 by Vishay Measurements Group via a Wheatstone bridge arrangement. The four transducers are connected to a DT300 Series data acquisition board by Data Translation, which is installed in a Dell Pentium *II* PC desktop computer. The system has a maximum sampling rate of 250 kHz.

Four channels are employed for monitoring the four transducers and the data is sampled at a rate of 62.5 kHz per channel. With more advanced, and expensive, equipment it is possible to sample all channels at a higher rate. The data acquisition system for the strain gauges and the accelerometer was triggered manually. The experimental configuration and set-up is illustrated in Figure 4.

Fig. 4. Experimental set-up

The data acquisition system is completed with HP VEE from Hewlett Packard enabling acquisition, storage and manipulation of the data. The interrogation system that was used to operate the FBGS has a resolution of 0.1 $\mu\varepsilon$/Hz. Two sensors were interrogated with a sample rate of 1 kHz resulting in a resolution of 4 $\mu\varepsilon$ per sample per sensor. The system is still under research and development and commercial reasons do not allow a detailed description to be presented in this paper.

IMPACT EXPERIMENTS

The objectives with the FBGS instrumentation were to detect and assess permanent damage induced by low velocity impacts. The experiments consisted of the following essential three points:

- detect the impact event on the composite panel under a BVID condition and compare the results obtained with the ones from the resistive strain gages and from C-scanning;
- using the readings from the FBGS evaluate the permanent damage in the composite laminates in the form of calculated residual strains and again compare with the other methods;
- compare the grating integrity in a worst case scenario where several successive impacts are performed on the same point concurrent with the optical fibre;

The test panels were clamped in a fixture designed so that the impactor struck close to their geometric centers about which the FOS sensors were embedded and the resistance strain gages bonded. Six impact responses were recorded simultaneously during each impact test. The recorded signals were from the (1) accelerometer, (2) three resistance strain gages and (3) two fibre Bragg grating sensors.

The tests were conducted using a weight of 0.359 kg while the height was varied to produce a range of incident kinetic energies. Four sets of experiments were conducted covering the BVID, the middle and the top impact energy as well as the worst-case scenario of cumulative impacts on the same spot ranging from the BVID up to the top impact energy. A set of preliminary tests showed that the BVID condition is represented by the energy level of 0.335 J. The middle and the top impact energies correspond to 1.673 J and 2.993 J energy levels respectively. In the cumulative impacts set the energy level ranged from 0.335 J to 2.993 J in 0.335 J increments. The BVID condition was used to investigate the FOS system sensitivity. The duration of the impact events ranged between 1.3-2.0 ms.

The data acquisition system and the developed interrogation system were sampling over a period of 5 seconds. The obtained data from the fibre optic sensors are in the form of wavelength (λ) as a function of time (t). The results obtained from the FBGS were compared with the ones obtained from the RSG and C-scanning.

EXPERIMENTAL RESULTS

The impact tests were undertaken in the speed range of 1.3557 and 4.0808 m/s as these were calculated from the kinetic energy equations. The effect of increasing impact energy on the laminates with the embedded FBGS is shown in Fig. 5. The force-time traces from the accelerometer represent the impacts of 0.335 J, 1.673 J and 2.993 J respectively. Increasing the impact energy to induce damage results in larger impact forces. In addition, high frequency oscillations are produced that start at shorter times and become larger with greater variations.

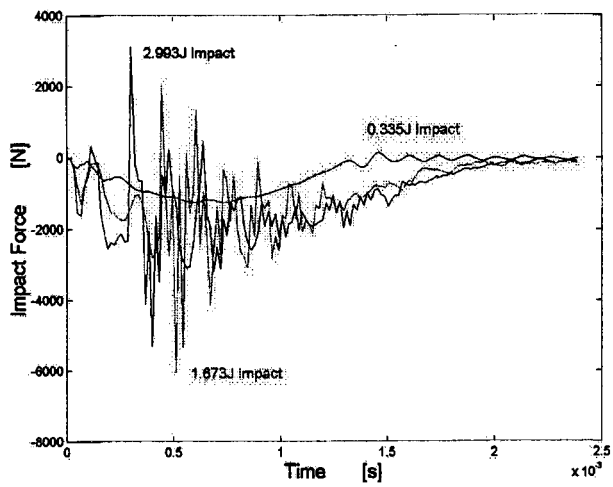

Fig. 5. Impact force versus time signal for three different impacts in CFRP's with embedded FBGS.

The above traces are very similar to the ones obtained from the laminates without FOS for the same impact conditions. The only difference is in the detected maximum impact forces due to slight variation in the impact location every time. The findings from the filtering process of the obtained impact data will be discussed in a future paper.

The strain traces for the BVID condition that were obtained from the two RSG are shown in Fig. 6. The stress waves that were produced from the impact are present for sometime until they get absorbed from the laminate. The central RSG did not provide data due to debonding. The RSG detect the impact event and provide dynamic strain data during the impact event but cannot assess the impact-induced internal damage of the composite test panel. Figure 7 presents the real-time detection of the impact and the shifting in the wavelength of the embedded FBGS after the impact manifesting the existence of internal damage.

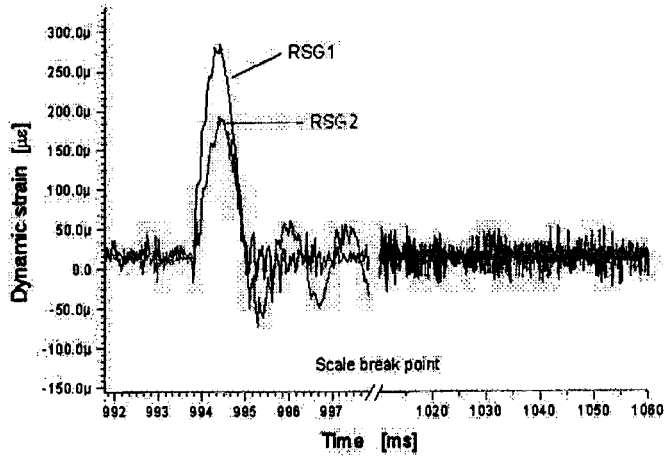

Fig.6. Detected transient strain from RSG for a 0.335 J impact

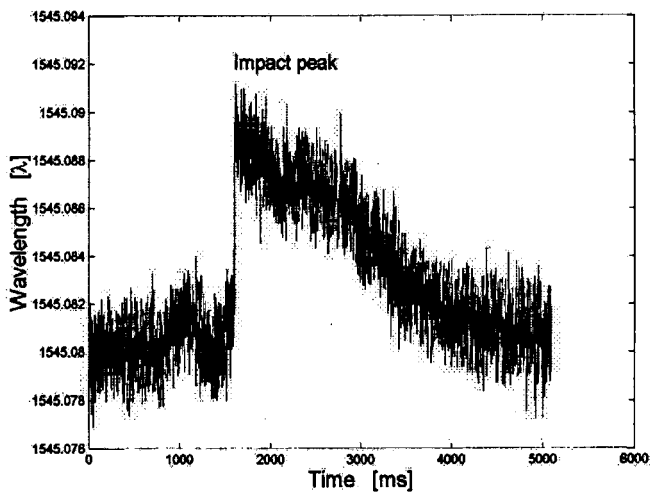

Fig. 7. Shift of wavelength during and after the impact event from FBGS no 2

The interrogation system recorded the operating wavelength of the FBGS as a function of time and by using the following equation the residual strains from the impact event are obtained:

$$Strain(\mu\varepsilon) = \frac{(\Delta\lambda)_{avg}}{1.2} \times 10^{-3} = \frac{(\lambda - \lambda_0)_{avg}}{1.2} \times 10^{-3} \qquad (1)$$

FBGS are also sensitive to temperature fluctuations with a sensitivity of 10^{-2} nm/K. We expect localised heating of the material due to adiabatic and friction mechanisms. However, this effect is believed to be small as the heating caused (K) is at least an order of magnitude smaller than the residual strain ($\mu\ \varepsilon$). Nevertheless this effect is more significant at lower impact energies when the residual strain is greatly reduced. However, if a long settling period is allowed the inherently conductive CFRP panel reaches thermal equilibrium and residual strains can be observed without interference from this effect. Further research into the accurate temperature compensation of obtained results will be performed in the future.

Figure 8 illustrates the calculated residual strain versus impact energy. The existence of residual

strains corresponds to impact-induced damage in the laminate. As the impact energy increases the detected residual strains from the FBGS and the RSG increase as well. While in the BVID condition the RSG were unable of measuring the residual strain, the interrogation system using the FBGS provided readings showing the existence of internal damage.

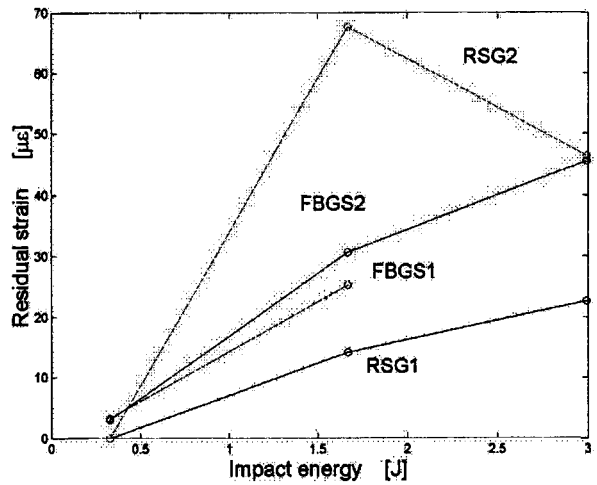

Fig. 8. Detected impact-induced damage in the form of calculated residual strains

It can be seen that the embedded FBGS experience different strains than the RSG as well as the RSG between them. The reason is that the RSG are located on the backside of the composite laminate where we expect to get higher transient strains. The out-of-trend RSG2 reading under a 1.673 J impact could be explained by electromagnetic interference from other lab equipment operating during the experimental tests. As it has already been mentioned the FOS are immune to EMI.

Using C-scans, we compared the impacted composite panels without embedded FBGS with the ones with the FBGS. The results agreed with the existing literature arguing that the presence of optical fibres had little or marginal effect on the shape and size of damage area, as well as on the host strain field of the laminate under the low-energy impact loads when the optical fibres were embedded parallel to the host reinforcing fibres [13-15] (Fig. 9,10).

However, it should be noted that the C-scans were unable of producing a clear picture of impact-induced internal damage in the composite laminate under the lowest impact of 0.335 J. Yet, the FBGS provided information about the damaged composite in the form of detected residual strain. This can be explained by the low resolution of the C-scan system that was employed to perform the task.

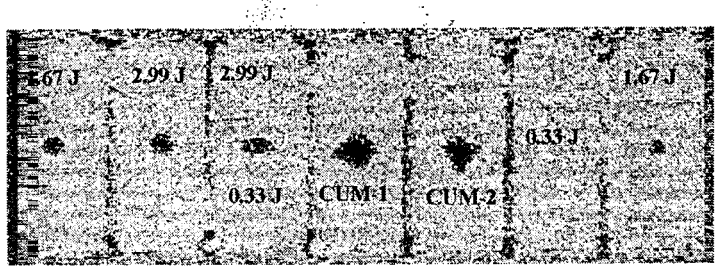

Fig. 9. C-scans of impacted CFRP's with embedded FBGS

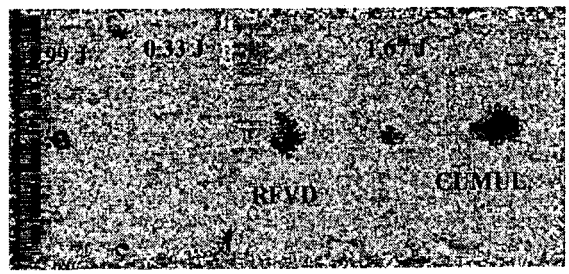

Fig. 10. C-scans of impacted CFRP's without FBGS

In Fig. 10 the delamination trace with the label RFVD was produced by successive impacts on a CFRP with the reinforcing fibres of the top layer oriented in a perpendicular direction when compared with the rest of the composite laminates. The delamination shape is slightly different than the typical shape produced by cumulative impacts.

CONCLUSIONS

The paper presented a study carried out in the University of Southampton into the detection and assessment of LVI on carbon fibre reinforced plastics (CFRP). A novel interrogation system developed at the Optoelectronics Research Centre and the Department of Engineering Materials using fibre Bragg grating sensors was employed. The experimental results from impact tests in composites validated and confirmed the high sensitivity and potentials of the developed system. The FBGS detected the impact event and produced readings of residual strains after the BVID test, while the resistive strain gages and the C-scanning method failed of doing so.

It seems clear that the step response in the FBGS wavelength readings induced from the impact event results in the calculated residual strains, which is a useful metric of internal damage. The obtained information can be related with the initiation and propagation of delaminations and matrix crackings providing a full and completed assessment of LVI in composite laminates. FOS are appropriate for damage assessment but there is a need for higher interrogation speed in order to have a complete trace of dynamic readings during the impact event from more than one sensors embedded in through-the-thickness of the composite laminate.

ACKNOWLEDGEMENTS

The help of Mr. E. Roszkowiak in the construction of the impact rig is gratefully acknowledged. The authors would also like to thank Mr. P. Williams for his helpful assistance during the various stages of the study.

REFERENCES

1. P. Pintado, T.J. Vogler and J. Morton, *Comp. Eng.* 1, (1991), p.195.
2. M. Lin and F.K. Chang, *Mat. Today*, 2, (1999), p.18.
3. M.V. Hosur, C.R.L. Murthy and T.S. Ramamurthy, *Proc. of the ASME, Noise Control and Acoustic Division*, NCA, 24, (1997), p.203.

4. M.O.W. Richardson and M.J. Wisheart, *Comp. Part A-Applied Sc. and Manuf.*, 27, (1996), p.1123.
5. C.C. Chang and J.S. Sirkis, *Smart Mat. & Str.*, 7, (1998), p.166.
6. D.A. Kersey, M.A. Davis, H.J. Patrick, M. LeBlanc, K.P. Koo, C.G. Askins, M.A. Putnam and E.J. Friebele, *J. of Light. Technol.*, 15, (1997), p.1442.
7. W.W. Morey, *Proc. SPIE Pacific Northwest Fibre Optic Sensor Workshop*, 2574, (1995), p.22.
8. C. Doyle, A. Martin, T. Liu, M. Wu, S. Hayes, P.A. Crosby, G.R. Powell, D. Brooks and G.F. Fernando, *Smart Mat. & Str.*, 7, (1998), p.145.
9. R.M. Measures, *Comp. Eng.*, 2, (1992), p.597.
10. G.P. Carman and G.P. Sendeckyj, *J. of Comp. Technol. Res.*, 17, (1995), p.183.
11. R.M. Measures, N.D.W. Glossop, J. Lymer, M. LeBlanc, J. West, S. Debois, W. Tsaw and R.C. Tennyson, *Applied Optics*, 28, (1989), p.2626.
12. N. Elvin, and C. Leung, *J. of Intel. Mat. Sys. and Struc.*, 8, (1997), p.824.
13. B.S. Jeon, J.J. Lee, J.K. Kim and J.S. Huh, *Smart Mat. & Str.*, 8, (1999), p.41.
14. J.S. Sirkis, C.C. Chang and B.T. Smith, *J. of Comp. Mat.*, 28, (1994), p.1347.
15. L. Tang, X. Tao and C.L. Choy, *Smart Materials & Structures*, 8, (1999), p.154.